Journal of the European Ceramic Society 22 (2002) 329–335

www.elsevier.com/locate/jeurceramsoc

# High temperature deformation of a 5 wt.% zirconia-spinel composite: influence of a threshold stress

Ahmed Addad, Jacques Crampon, Richard Duclos*

*Laboratoire de Structure et Propriétés de l'Etat Solide, ESA 8008, Bât. C6, Université des Sciences et Technologies de Lille, 59655 Villeneuve d'Ascq Cedex, France*

Received 16 November 2000; received in revised form 13 April 2001; accepted 21 April 2001

**Abstract**

Creep experiments performed on a 5 wt.% zirconia- $MgAl_2O_4$ spinel material, in the stress and temperature ranges 8–200 MPa and 1350–1410°C, have shown the importance of grain boundaries in deformation of this material. Deformation can be analysed as the result of two sequential contributions. At low stress, an increase in the apparent stress exponent and the occurrence of a threshold stress, whose value roughly varies inversely proportional to spinel grain size, were observed. At high stress, grain boundary diffusion is the most likely mechanism that controls the grain boundary sliding. These observations are consistent with previous experiments showing that sliding of spinel/spinel boundaries is more difficult than sliding of spinel/zirconia boundaries in the low stress range. The plastic flow is analysed by means of grain boundary dislocations whose density increases with stress. At low stress, when the density of boundary dislocations is low, creep rates are interface-controlled while at high stress, when the boundary dislocation density is large, rates are limited by the long-range diffusion process. 

*Keywords:* Composites; Creep; Grain boundaries; Interfaces; $MgAl_2O_4/ZrO_2$; Spinel

## 1. Introduction

High temperature deformation of ceramic materials is largely dependent on grain boundaries, specially when a fine grain size (lower than 1 μm) impedes intragranular dislocation slip. Then deformation takes place by grain boundary sliding and a connected accommodation mechanism. These mechanisms lead to values of the stress exponent n in the relation:

$$\dot{\varepsilon} = \alpha(\sigma/\sigma^*)^n \quad (1)$$

with $\dot{\varepsilon}$ the strain rate, $\sigma$ the stress, $\sigma^*$ a reference stress and $\alpha$ a reference strain rate, that typically range between 1 and 3 for a large number of ceramics,[1–3] depending on stress, material purity and grain size.

Sometimes, when low stresses are applied, the stress exponent can reach high values, far above 3. These exponent values are interpreted in terms of an effective stress defined as $(\sigma - \sigma_0)$ where $\sigma_0$ is a threshold stress, i.e. a lower limit for any measurable plastic flow.[4] Frequently observed in metal matrix composites,[4] several examples of a threshold have also been reported in ceramic materials: alumina,[5] SiC(w) reinforced alumina/zirconia composites,[6,7] high purity zirconia polycrystals[8] or spinel materials[9] with a very fine grain size (30–100 nm). The threshold stress may be related for instance to the presence of impurities or precipitates at grain boundaries,[10,11] the fluctuation of grain boundary dislocation length[12] or more complex origins.[9]

The present work is concerned with the study of the plastic deformation of a spinel/zirconia composite for which such a behaviour, which can be explained in terms of a threshold stress, was noted. In addition, an interface-controlled diffusion creep, likely to be related to grain boundary dislocations, was ascertained.

## 2. Experimental procedure

The material used in this study contains 5 wt.% of zirconia particles (about 3.2 vol.%). It was fabricated by zirconia sol gel coating of crystalline $MgAl_2O_4$ spinel particles (Baikowski S30CR, Annecy, France), according

* Corresponding author. Tel.: +33-3-2043-4990; fax: +33-3-2043-6591.

*E-mail address:* richard.duclos@univ-lille1.fr (R. Duclos).

0955-2219/01/$ - see front matter 
PII: S0955-2219(01)00297-7

to a technique already described.[13] The main impurities in the spinel powder, given by the supplier, are (in wt. ppm): Na: 10, K: 200, Fe: 20, Si: 50 and Ca: 30. Disks of the dried and fired powder mixture were cold pressed and sintered at 1550°C for 1 h, leading to a density near the theoretical one (about 99.4%). Besides, this fabrication method allowed us to achieve a very homogeneous distribution of zirconia grains in the spinel matrix as Fig. 1 shows. Grains of the two phases are mainly equiaxed and generally dislocation free. As-sintered specimens have grain sizes of $d_S = 0.87$ μm and $d_Z = 0.35$ μm for spinel and zirconia, respectively.

Creep tests were performed in compression in air at 1350, 1380 and 1410°C at stresses ranging from 8 to 200 MPa for the as-sintered material. Specimens had dimensions of 3×3×7 mm. Some tests were also experimented at 1380°C on annealed specimens ($d_S = 1.5$ μm; $d_Z = 0.4$ μm) to account for the effect of grain size on plastic flow. In a first step the stationary creep rate $\dot{\varepsilon}$ was analysed according to the classical high temperature deformation relationship:

$$\dot{\varepsilon} = K(s)\sigma^n d^{-p}\exp(-Q/\mathrm{RT}) \quad (2)$$

with $K(s)$ a structural parameter, $n$ the stress exponent, $p$ the grain size exponent and $Q$ the creep activation energy.

In addition to mechanical characterisation, microstructure examination prior to and after creep tests was conducted by scanning and transmission electron microscopy to examine the changes in grain sizes and shapes connected to the deformation.

## 3. Results

Creep curves were characterised by a very short transient creep followed by a steady state until the test completion (true strain higher than 60% in certain cases). Fig. 2 shows the effect of stress on the stationary creep rate at the three test temperatures. The curves are very similar, exhibiting a continuous decrease in the stress exponent n when stress increases. Fig. 3 shows the values of $n$, determined by the stress jump technique, a more accurate method than the direct comparison of creep rates of different specimens. At low stress, $n$ is higher than 4 and diminishes to about 1.5 at 200 MPa depending slightly on material grain sizes and test temperature.

The effect of temperature on creep rate, estimated from the measurement of the activation energy $Q$, is strongly dependent on stress too. The activation energy

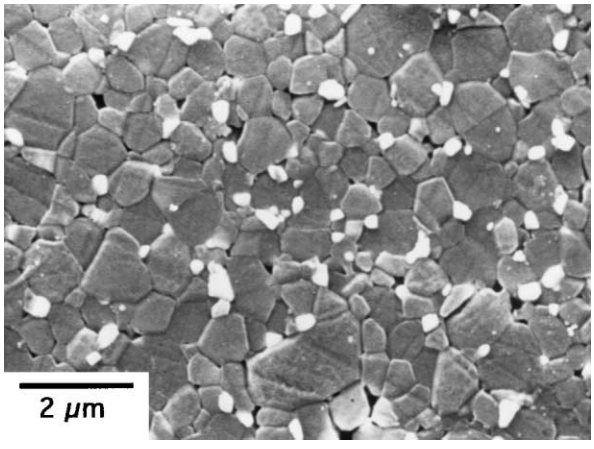


Fig. 1. SEM micrograph of an as-sintered specimen. The distribution of zirconia grains in the spinel matrix is homogeneous.

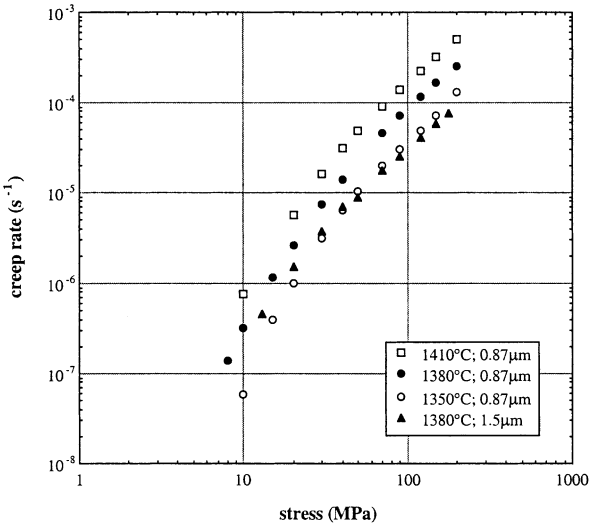


Fig. 2. Variation of creep rate with stress for as-sintered specimens ($d = 0.87$ μm) tested at 1350, 1380 and 1410°C and for annealed specimens ($d = 1.5$ μm) tested at 1380°C.

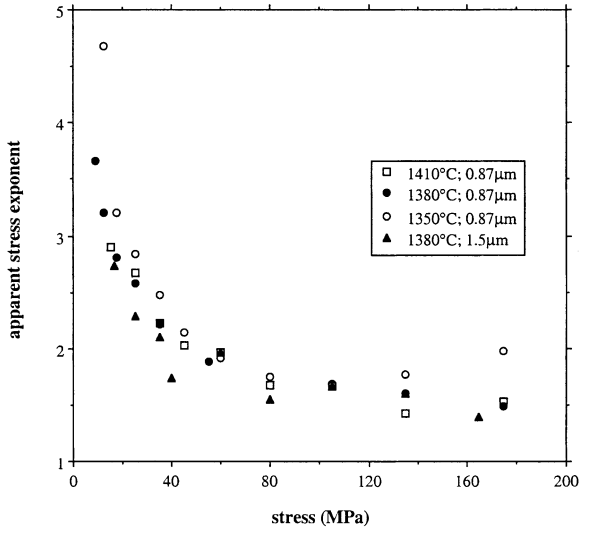


Fig. 3. Variation of the stress exponent with stress for all the experimental conditions.

value is about 600 kJ mol$^{-1}$ at 100 MPa and reaches more than 1000 kJ. mol$^{-1}$ at 10 MPa.

The influence of grain size on the creep rate at 1380°C is perceptible in Fig. 2. Interpreted in terms of a grain size exponent [defined as $p = \text{Ln}\,(\dot{\varepsilon}(0.87\ \mu\text{m})/\dot{\varepsilon}(1.5\ \mu\text{m}))/\text{Ln}\,(1.5/0.87)$], it corresponds to values of $p$ increasing with stress from 0.56 at 13 MPa to 2 at 180 MPa (Table 1).

Comparatively, the microstructure evolution with deformation was weak and not really connected to stress, except for cavity formation. Grains kept an equiaxed shape and dislocations were rarely observed inside grains. Deformation-induced cavities, observed for the highest stresses (Fig. 4), were mainly located at triple points and sometimes elongated between spinel grains. However, density decrease never exceeded 2% even in the most unfavourable conditions at 200 MPa for true strains of about 70%.

## 4. Discussion

### 4.1. Creep parameter analysis

The above-mentioned results show a strong influence of stress on the various experimental thermomechanical parameters, the stress exponent $n$, the activation energy $Q$ and the grain size exponent $p$. That observation could be explained by the existence of several concurrent mechanisms. Nevertheless, at the lowest stresses the exponent $n$ is well above the values that can be reasonably expected for a diffusion accommodated creep, the most probable deformation mode, and consequently data were re-examined in terms of a threshold stress by replacing in relation (2) the applied stress $\sigma$ by an effective stress $(\sigma - \sigma_0)$. The values of the threshold stresses $\sigma_0$ and the exponent $n$, related now to the effective stress, were estimated by plotting $\dot{\varepsilon}^{1/n}$ against $\sigma$ for the most likely values of $n$.[14] To this purpose, only the rates at low stress (below 40 or 50 MPa) were used because they are the most affected by the threshold. The best agreement was obtained for $n = 2$. It is presented in Fig. 5a, a plot of $\dot{\varepsilon}^{1/2}$ versus stress, that shows linear relations between the two variables, the intersection with the abscissa axis giving the threshold value. The thresholds, listed in Table 2, slightly decrease with increasing temperature and grain size. This latter

Table 1
Influence of stress on the experimental value of the grain size exponent

| Stress (MPa) | 13 | 20 | 30 | 40 | 70 | 90 | 120 | 150 | 180 |
|---|---|---|---|---|---|---|---|---|---|
| $p$ | 0.56 | 1.01 | 1.27 | 1.3 | 1.77 | 1.9 | 1.91 | 1.91 | 2 |

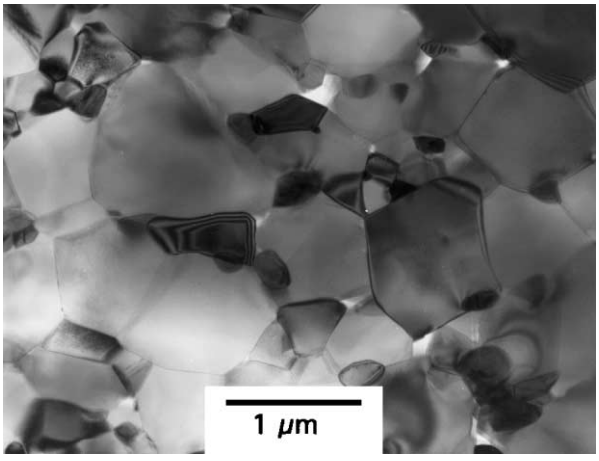


Fig. 4. Transmission electron micrograph of a specimen deformed at 1380°C under stresses of 120, 150 and 200 MPa up to a true strain of 32% that shows the cavity nucleation at triple points and the retention of equiaxed grain structure.

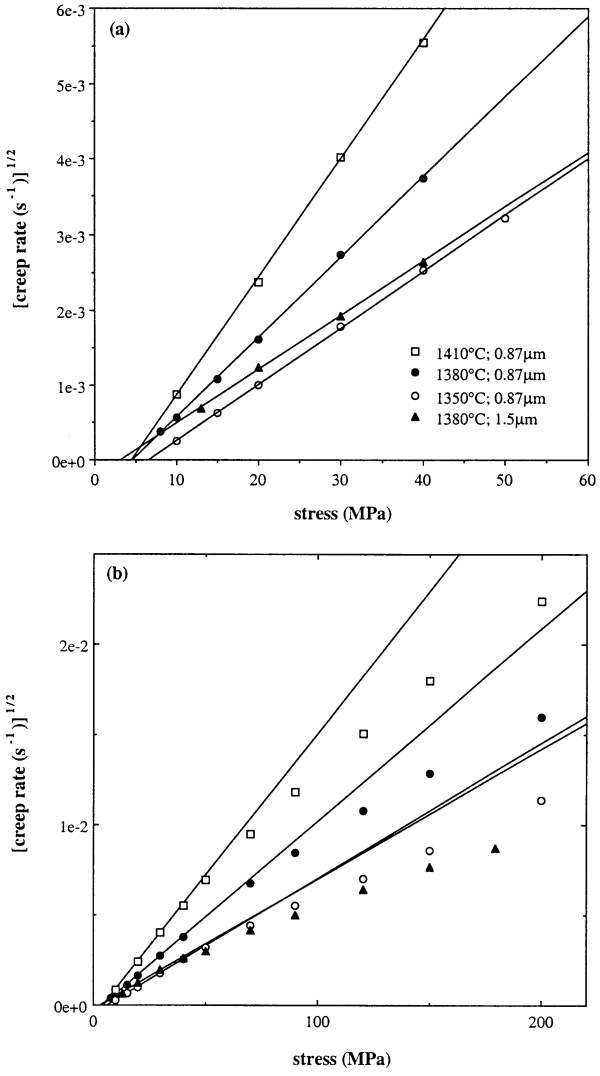


Fig. 5. (a) Variation at low stress of $\dot{\varepsilon}^{1/2}$ with stress for determining the threshold stress and the coefficient $A$ in relation (3). $A^{1/2}$ is the slope of the linear interpolates; (b) the same plot as (a) when all the data are taken into account.

Table 2
Threshold stress as determined in Fig. 5 as a function of temperature (1st line) and spinel grain size (2nd line); the fourth and fifth lines report the value of the coefficients A and B of the low and high stress relations (3) and (4), respectively

| Temperature (°C) | 1350 | 1380 | 1410 | 1380 |
|---|---|---|---|---|
| $d$ (μm) | 0.87 | 0.87 | 0.87 | 1.5 |
| Threshold stress (MPa) | 6.6 | 4.7 | 4.5 | 3.3 |
| $A$ ($10^{-8}$ $s^{-1}$ $MPa^{-2}$) | 0.56 | 1.13 | 2.46 | 0.52 |
| $B$ ($10^{-6}$ $s^{-1}$ $MPa^{-1}$) | 1.7 | 3.1 | 6.9 | 0.78 |

observation suggests that the threshold stress is a decreasing function of the grain size, in agreement with several theoretical models[11,12,15] or experimental results[8] and consequently the low stress rates $\dot{\varepsilon}_{ls}$ has been described through a relation of the form:

$$\dot{\varepsilon}_{ls} = A(\sigma - \sigma_0)^2 = A(\sigma - \phi/d)^2 \quad (3)$$

where $A$ is independent of stress and $d$ is the spinel grain size. Due to the low zirconia content in this material, the effect of grain size was assumed to depend mainly on spinel matrix. The various values of $A$, $A^{1/2}$ being the slope of the straight lines in Fig. 5a, are presented in Table 2. A value of $\phi$ of about 3.9 MPa μm was obtained at 1380°C.

When all the experimental stresses are taken into consideration (Fig. 5b), it is obvious that the whole points cannot be described by a single power law, supporting the assumption that another mechanism operates at high stress. The stress exponent values ranging from 1.4 to 1.8 above 70 MPa (see Fig. 3) suggest that the most likely mechanism is a newtonian one, with a stress exponent of 1, linking the high stress rates $\dot{\varepsilon}_{hs}$ to stress through the expression:

$$\dot{\varepsilon}_{hs} = B\sigma \quad (4)$$

with $B$ a parameter describing the grain size and temperature effects. The shape of the $\dot{\varepsilon}(\sigma)$ curves indicates that the two mechanisms are sequential ones. Consequently, the resultant creep rates $\dot{\varepsilon}$ are related to low and high stress rates by:

$$\dot{\varepsilon} = (\dot{\varepsilon}_{ls} \times \dot{\varepsilon}_{hs})/(\dot{\varepsilon}_{ls} + \dot{\varepsilon}_{hs}) \quad (5)$$

The $B$ values were determined from relation (5) and from the rates measured for the highest stresses; they are presented in Table 2. These values depend explicitly on grain size and temperature.

At first the effect of grain size on creep rate at 1380°C was determined by comparing the values of coefficients $A$ and $B$ for an as-sintered specimen ($d = 0.87$ μm) and an annealed one ($d = 1.5$ μm). To this end $A$ and $B$ in relations (3) and (4) were assumed to depend on grain size as:

$$A(\text{or } B) = A^*(\text{or } B^*)/d^p \quad (6)$$

with $A^*$ and $B^*$ coefficients related to temperature only. Values of $p = 1.44$ and $p = 2.5$ were obtained for the low stress and high stress rates, respectively. In order to refine the values of $p$, the variation of the apparent grain size exponent against stress was calculated by considering that $p$ could be equal to 1 or 2 at low stress and to 2 or 3 at high stress and by using Eqs. (3), (4) and (5) and the values of $A$ and $B$ in Table 2. The result is presented in Fig. 6 in which $a$ and $b$ stand for $p$ in the low and high stress laws, respectively. The best agreement is obtained for creep rates proportional to the grain size inverse at low stress and to the cubic grain size inverse at high stress.

At low stress, the grain size dependence of the threshold is responsible for the decrease in the apparent grain size exponent while at high stress, the fine grain size of the material renders the low stress mechanism still active and induces an apparent grain size exponent located between the low and high stress exponents.

Finally, the true activation energies of low and high stress mechanisms have been calculated from the values of $A$ and $B$ in Table 2 assuming the effect of temperature in $A$ and $B$ terms to be:

$$A(\text{or } B) = A^{**} \text{ (or } B^{**})\exp(-Q/\mathrm{RT}) \quad (7)$$

in which $A^{**}$ and B** are structure parameters independent of temperature. Data lead to activation energies of 560 and 620 kJ $mol^{-1}$ at low stress and high stress, respectively, values close to the energy determined at high stress. Owing to the large incertitude that affects the determination, it is not possible to assert

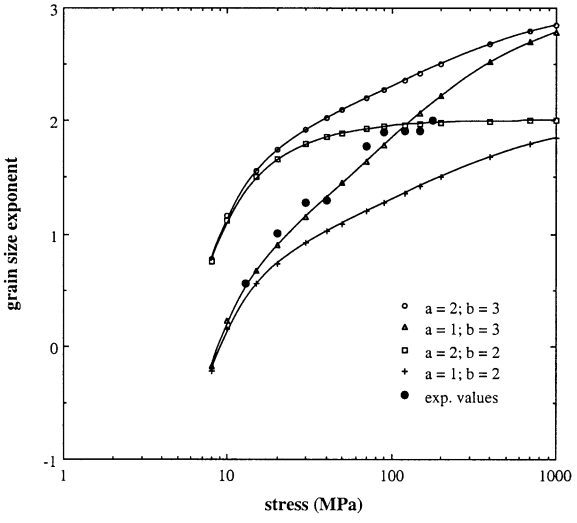


Fig. 6. Variation of the experimental value of the grain size exponent with stress by considering various possibilities for the grain size exponent at low stress ($a = 1$ or 2) and at high stress ($b = 2$ or 3). The best agreement corresponds to $a = 1$ ($\dot{\varepsilon}$ proportional to $d^{-1}$ in the low stress relationship) and b = 3 ($\dot{\varepsilon}$ proportional to $d^{-3}$ in the high stress relationship).

these two values are really different. They are well above the activation energy reported by Panda et al. ($460 \pm 50$ kJ mol$^{-1}$)[16] or the energy for lattice diffusion of oxygen ions ($443 \pm 50$ kJ mol$^{-1}$),[17,18] believed to be the slowest diffusing species in spinel. They are close to the activation energy reported by Beclin et al.[19] (about 600 kJ mol$^{-1}$) for creep of spinel polycrystals with a matrix grain size of 0.6 μm.

The above analysis suggests that relations (3) and (4) can be rewritten as a function of stress, grain size and temperature:

$$\dot{\varepsilon}_{ls} = C_1[\sigma - \sigma_0(T, d)]^2 d^{-1} \exp\left(-560 \times 10^3/\mathrm{RT}\right) \quad (8)$$

$$\dot{\varepsilon} = C_2 \sigma d^{-3} \exp\left(-620 \times 10^3/\mathrm{RT}\right) \quad (9)$$

with $C_1 = 2 \times 10^{-18}$ MPa$^{-2}$ μm s$^{-1}$, $C_2 = 2.5 \times 10^{-20}$ MPa$^{-1}$ μm$^3$ s$^{-1}$, $\sigma$ and $d$ being expressed in MPa and μm, respectively. Using these relations and (5), all the data in Fig. 2 have been normalized to a grain size of 0.87 μm and a temperature of 1380°C. The results, presented in Fig. 7 as a plot of the normalized creep rate against stress, show a good accordance between the various experimental conditions.

### 4.2. Interpretation

Analysis of experimental results showed they could be interpreted by considering (i) a threshold stress and (ii) two sequential deformation processes. Structure evolution was weak and did not show distinct features according to stress. Besides, in a recent work concerned with the study of grain boundary sliding in a spinel-zirconia composite (20 vol.% of zirconia),[20] the role of this sliding as the main origin of deformation has been well demonstrated. It is probable that this conclusion is still valid in the present case. The deformation issues from grain boundary sliding and a diffusion accommodation process in comparison with activation energies. The low stress activation energy, that is much higher than those measured for lattice diffusion, and the narrow difference between the two activation energy values suggest that a same diffusion process could be active throughout the experimental stress range, i.e. grain boundary diffusion owing to the high stress flow equation.

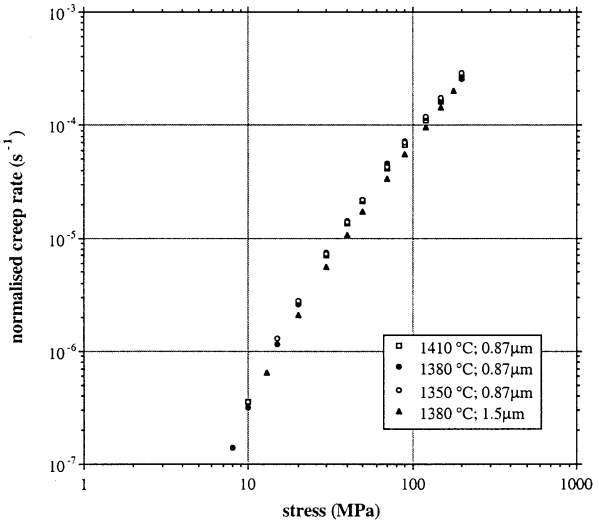


Fig. 7. Variation with stress of the creep rate normalised by the temperature (reference temperature = 1380°C) and the grain size (reference grain size = 0.87 μm) for all the experimental conditions. Normalised rates were calculated using Eqs. (5), (8) and (9) and data in Table 2.

The above creep behaviour can be described by considering that grain boundaries are not perfect sources or sinks for vacancies contrary to assumptions of classical diffusion creep models.[21–23] Vacancies are emitted or absorbed by discrete sources or sinks: the grain boundary dislocations. The resultant modifications on the creep behaviour have been analysed by Arzt et al.[12] These authors used an expression of the boundary dislocation density $\rho$ proposed by Burton:[15]

$$\rho = \sigma/2\mu b_{gb} \quad (10)$$

with $\mu$ the shear modulus of the material and $b_{gb}$ the Burgers' vector of grain boundary dislocations. This relation is the planar equivalent of the equation giving the intragranular dislocation density. The creep rate $\dot{\varepsilon}$ resulting from that density is:

$$\dot{\varepsilon} = \rho b_n v/d \quad (11)$$

where $b_n$ is the component of $b_{gb}$ normal to the grain boundary plane, $d$ is the grain size and $v$ is the dislocation velocity related to stress and mobility $M$ by:

$$v = \sigma b_n M \quad (12)$$

If it is assumed, in the absence of any obstacles to dislocation displacement, that their mobility is intrinsic, i.e.: $M = D_{gb}b/kT$ with $D_{gb}$ the grain boundary diffusivity, then the resultant creep rate is about:

$$\dot{\varepsilon} = bb_n D_{gb}\sigma^2/2kT\mu d \quad (13)$$

At low stress, when the boundary dislocation density is small, the number of emission/annihilation sites is weaker than in a continuum model and consequently the related creep rate is lower than in the classical Coble model.[23] Creep rates are then controlled by the motion of a reduced number of grain boundary dislocations. The experimental rates proportional to $\sigma^2$ and $d^{-1}$ in this stress range are in good agreement with that deduced from relation (13).

As stresses increase, grain boundary dislocation density is higher and higher. Under these conditions the

number of sources/sinks becomes high enough in order that creep rate is now limited by the diffusive transport of matter between sources and sinks as in Coble creep.[23] Consequently the stress exponent should decrease to 1 at high stress. The non observation of a stress exponent of 1 originates from the fine grain sizes of the specimens that favour the contribution of the low stress process and allow us to observe only, at the highest experimentally applied stresses, a transient behaviour between the two limiting conditions. The two processes, creation of grain boundary dislocation and diffusive transport of matter, are necessary and the resultant creep rate can be written as:[12]

$$\dot{\varepsilon}^{-1} = \dot{\varepsilon}_{\text{diff}}^{-1} + \dot{\varepsilon}_{\text{disl}}^{-1} \tag{14}$$

expression equivalent to that proposed in relation (5).

This description of the plastic flow, that corresponds to the two steps of a same transport process, does not imply changes in microstructure or in activation energy with stress. The main difference that exists between the low and high stress behaviours lies in the grain boundary capability to absorb/emit vacancies in connection to grain boundary dislocation density. As boundary sliding and diffusion accommodation are linked by the movement of boundary dislocations,[10] a decrease in their density should entail a related decrease in sliding capacity of the boundary. This assumption is supported by the study of Addad et al.[20] that showed a decrease in the sliding capacity of spinel–spinel interfaces relative to that of spinel–zirconia interphase boundaries in a spinel–zirconia composite when low stress levels were experimented.

Finally the magnitude of the threshold stress (a few MPa) is in agreement with the value that can be deduced from the relation proposed by Arzt et al.:[12]

$$\sigma_0 = 0.5\mu b_{\text{gb}}/d \tag{15}$$

Values of $\mu = 10^2$ GPa and $b_{\text{gb}} = 0.1$ nm (about one third of a lattice dislocation Burgers' vector[12]) leads to a threshold of 5.9 MPa. This threshold corresponds to energy fluctuation associated to the variation of grain boundary dislocation length.

In a recent report, Berbon and Langdon[24] studied the origin of the change in stress exponent with stress [3 at low stress (a few MPa) and 2 at high stress (250 MPa)] during the high temperature deformation of a 3 mol% yttria stabilised zirconia.[25] Though our analysis is different from that proposed by these authors, the arguments that are put forward are comparable. Thus, Berbon and Langdon described the whole $\dot{\varepsilon}(\sigma)$ curve from a modified Coble creep model in which the role of grain boundary dislocations, as discrete sources or sinks for vacancies, is taken into account according to the model of Arzt et al.[12] Unless the creep rate is expressed by a single relation, and not a combination of two, this model can be described by two sequential processes. The first one corresponds to the diffusive transport of matter and the second one (through the term implying the number of dislocations in a grain boundary) to the effect of dislocation density on the creep rate. Considering that the grain boundary dislocation density increases with stress, limiting conditions of $n = 1$ and $p = 3$ at the highest stresses (analogous to Coble creep) and $n = 3$ and $p = 1$ at the lowest stresses were obtained. Owing to the fine grain size of the zirconia (0.41–1.2 μm) the creep was mainly interface-controlled, even at high stress, and a newtonian flow with $n = 1$ was not observed over the range of applied stresses. However, unlike our assumption, these authors did not believe that grain boundary sliding, as a deformation process, was a viable process under the experimental conditions.

## 5. Conclusions

Creep experiments performed on a 5 wt.% zirconia–spinel composite have emphasised the existence of a threshold stress and its consequences on the determination of the flow relationship. If grain boundary sliding is likely to contribute to a large part of deformation, the low stress creep rates are limited by a small grain boundary dislocation density. The emission or absorption of vacancies is then lower than in the classical creep models and creep is interface-controlled. At high stress, with the increase in boundary dislocation density, the stress and grain size exponents suggest that a classical Coble creep took place progressively. These two deformation contributions are sequential and related to the same grain boundary diffusion energy. This interpretation is consistent with the experimental observations showing that activation energies and microstructures of strained specimens are virtually independent of stress.

The influence of the zirconia particle content on the plastic flow is currently analysed. This should allow us to improve the understanding of (i) the role of the two major kinds of grain boundary concerning the macroscopic deformation of composites, (ii) the matter diffusion process and (iii) the low stress behaviour, finer grain sizes, favouring the effect of the threshold stress, being generated when the zirconia ratio is increased.

## Acknowledgements

The authors gratefully acknowledge A. Dauger and R. Guinebretière (ENSCI Limoges, France) for supplying and help in fabrication of the materials used in this study. This work was partially supported by the French "Région Nord-Pas de Calais" and the Fonds Européen de Développement Régional (Feder).

## References


1. Chen, I.-W. and Xue, L. A., Development of superplastic structural ceramics. *J. Am. Ceram. Soc.,* 1990, **73**, 2585–2609.
2. Chokshi, A. H., Superplasticity in fine grained ceramics and ceramic composites: current understanding and future prospects. *Mater Sci. Eng.,* 1993, **A166**, 119–133.
3. French, J. D., Zhao, J., Harmer, M. P., Chan, H. M. and Miller, G. A., Creep of duplex microstructures. *J. Am. Ceram. Soc.,* 1994, **77**, 2857–2865.
4. Li, Y. and Langdon, T. G., A unified interpretation of threshold stresses in creep and high strain rate superplasticity of metal matrix composites. *Acta Mater.,* 1999, **47**, 3395–3403.
5. Cannon, R. M., Rhodes, W. H. and Heuer, A. H., Plastic deformation of fine-grained Alumina ($Al_2O_3$): I, interface-controlled diffusional creep. *J. Am. Ceram. Soc.,* 1980, **63**, 46–53.
6. Duclos, R. and Crampon, J., Diffusional creep of a SiC whisker reinforced alumina/zirconia composite. *Scripta Metall.,* 1989, **23**, 1673–1678.
7. Backhaus-Ricoult, M. and Eveno, P., Creep properties of an alumina-zirconia composite reinforced with silicon carbide whiskers. *J. Eur. Ceram. Soc.,* 1993, **11**, 51–62.
8. Bravo-Léon, A., Jiménez-Melendo, M. and Dominguez-Rodriguez, A., The role of a threshold stress in the superplastic deformation of fine-grained yttria-stabilized zirconia polycrystals. *Scripta Mater.,* 1996, **34**, 1155–1160.
9. Lappalainen, R., Pannikat, A. and Raj, R., Superplastic flow in a non-stoichiometric ceramic: magnesium aluminate spinel. *Acta Metall. Mater.,* 1993, **41**, 1229–1235.
10. Ashby, M. F., Boundary defects and atomistic aspects of boundary sliding and diffusional creep. *Surface Sci.,* 1972, **21**, 498–542.
11. Ashby, M. F. and Verrall, R. A., Diffusion-accommodated flow and superplasticity. *Acta Metall.,* 1973, **21**, 149–163.
12. Artz, E., Ashby, M. F. and Verrall, R. A., Interface controlled diffusional creep. *Acta Metall.,* 1983, **31**, 1977–1989.
13. Guinebretière, R., Masson, O., Ruin, P., Trolliard, G. and Dauger, A., Sol gel coating of ceramic powders. *Phil. Mag. Let.,* 1994, **70**, 389–396.
14. Lagneborg, R. and Bergman, B., The stress/creep rate behaviour of precipitation-hardened alloys. *Metal Sci.,* 1976, **10**, 20–28.
15. Burton, B., Interface reaction controlled diffusional creep: a consideration of grain boundary dislocation climb sources. *Mater. Sci. Eng.,* 1972, **10**, 9–14.
16. Panda, P. C., Raj, R. and Morgan, P. E. D., Superplastic deformation in fine-grained $MgO{\cdot}2Al_2O_3$ spinel. *J. Am. Ceram. Soc.,* 1985, **68**, 522–529.
17. Reddy, K. P. R. and Cooper, A. R., Oxygen diffusion in magnesium aluminate spinel. *J. Am. Ceram. Soc.,* 1981, **64**, 368–371.
18. Ando, K. and Oishi, Y., Effect of ratio of surface area to volume on oxygen self diffusion coefficients determined for crushed MgO–$Al_2O_3$ spinels. *J. Am. Ceram. Soc.,* 1983, **6**, C–131-C-13219.
19. Béclin, F., Duclos, R., Crampon, J. and Valin, F., Microstructural superplastic deformation in MgO–$Al_2O_3$ spinel. *Acta Metall. Mater.,* 1995, **43**, 2753–2760.
20. Addad, A., Crampon, J., Guinebretière, R., Dauger, A. and Duclos, R., Grain boundary sliding in a 30 wt% zirconia–spinel composite: influence of stress. *J. Eur. Ceram. Soc.,* 2000, **20**, 2063–2068.
21. Nabarro, F. R. N., Deformation of crystals by the motion of single ions. In *Report of a Conference on Strength of Solids*, Bristol 1947. The Physical Society, London, 1948, pp. 75–90.
22. Herring, C., Diffusional viscosity of a polycrystalline solid. *J. App. Phys.,* 1950, **21**, 437–445.
23. Coble, R. L., A model for boundary diffusion controlled creep in polycrystalline materials. *J. App. Phys.,* 1963, **34**, 1679–1682.
24. Berbon, M. Z. and Langdon, T. G., An examination of the flow process in superplastic yttria-stabilized tetragonal zirconia. *Acta Mater.,* 1999, **47**, 2485–2495.
25. Owen, D. and Chokshi, A. H., The high temperature mechanical characteristics of superplastic 3 mol% yttria stabilized zirconia. *Acta Mater.,* 1998, **46**, 667–679.